PERGAMON

Journal of Structural Geology 23 (2001) 1429–1440

JOURNAL OF STRUCTURAL GEOLOGY

www.elsevier.com/locate/jstrugeo

Microstructures, textures and deformation mechanisms in hematite

Carlos A. Rosière[a,*], Heinrich Siemes[b], Horst Quade[c], Heinz-Günter Brokmeier[d], Eleonore M. Jansen[d]

[a]*CPMTC/IGC/UFMG-Av. Antonio Carlos 6627, 31270-901, Belo Horizonte, MG, Brazil*
[b]*Institut für Mineralogie und Lagerstättenlehre, RWTH Aachen, Wüllnerstr 2, 52056 Aachen, Germany*
[c]*Institut für Geologie und Paläontologie, TU Clausthal, Leibnizstr. 10, 38678 Clausthal Zellerfeld, Germany*
[d]*GKSS Forschungszentrum Geesthacht GmbH, Max-Planck-Strasse, 21502 Geesthacht, Germany*

Received 10 November 1999; accepted 12 December 2000

Abstract

Deformation and recrystallization of hematite in iron formations and high-grade ore bodies of the Cauê Formation from the Quadrilátero Ferrífero District, Minas Gerais, Brazil, resulted in several types of fabrics, depending on the tectonic and metamorphic imprint. The fabrics vary from randomly oriented granoblastic to strongly oriented lepidoblastic/mylonitic with local development of cataclastic features.

Complete pole figures of the crystallographic planes (003)-basal plane; {110}-prism and {104}-rhombohedron were measured on several samples from different areas by means of neutron diffraction revealing a typical crystallographic preferred orientation for the different fabric types. The configuration and intensity of the maxima are directly related to the magnitude of the deformation and the type of response of the ore.

The analysis of the textures and microstructures of the iron ores and comparison with experimental deformation data lead us to the conclusion that three main mechanisms are active: basal slip, diffusion processes and anisotropic grain growth. Post-tectonic recrystallization and secondary grain growth did not affect the textures developed during deformation.

1. Introduction

The influence of tectonic structures on the concentration of iron-rich ore bodies in the metamorphic banded iron formations (BIF) of the Quadrilátero Ferrífero (Iron Quadrangle) has puzzled geologists for quite some time (Guild, 1957; Dorr, 1965). Most models have failed to develop a consistent structural analysis and to correlate the internal structures of the BIFs to the regional deformational picture, partly due to the poor understanding of their mechanical behavior. Softening of the banded iron formation is strongly influenced by the development of a crystallographic preferred orientation in hematite, due to effects of temperature, pressure, strain rate and fluid content on the deformation process.

During metamorphism and deformation, iron formations from the Quadrilátero Ferrífero have undergone a thorough oxidation process with increasing content of hematite and the development of a crystallographic preferred orientation (CPO). The texture (CPO) of hematite is due not only to its crystal-plastic deformation behavior, but also to syn-deformational growth of platy specularite crystals at the expense of magnetite (Hackspacher, 1979; Rosière, 1981; Guba, 1982; Lagoeiro, 1998).

To describe the textures and understand the processes involved not only helps to unveil the apparent complexity of the structures, but also facilitates an interpretation of the kinematic and deformational scenario in order to support structural analysis. The influence of the deformation on the generation of high-grade ore bodies can also be better studied and understood.

This study presents the results of microstructural and textural analysis in the iron formations from the Quadrilátero Ferrífero by comparing them with those from experimental studies (Hennig-Michaeli, 1977; Hennig-Michaeli and Siemes, 1982; Siemes et al., 1999a; Siemes and Klinkenberg, 2000). Most of the field work was accomplished at 15 open-cast ore deposits, located in different structural domains representing different degrees of deformation and metamorphism. This study illustrates the different types of microstructures and textures, shows how they change regionally, and presents hypotheses for the active mechanisms and processes operative during deformation.

* Corresponding author. Fax: +55-31-499-4440.
E-mail address: crosiere@dedalus.lcc.ufmg.br (C.A. Rosière).

0191-8141/01/$ - see front matter
PII: S0191-8141(01)00009-8

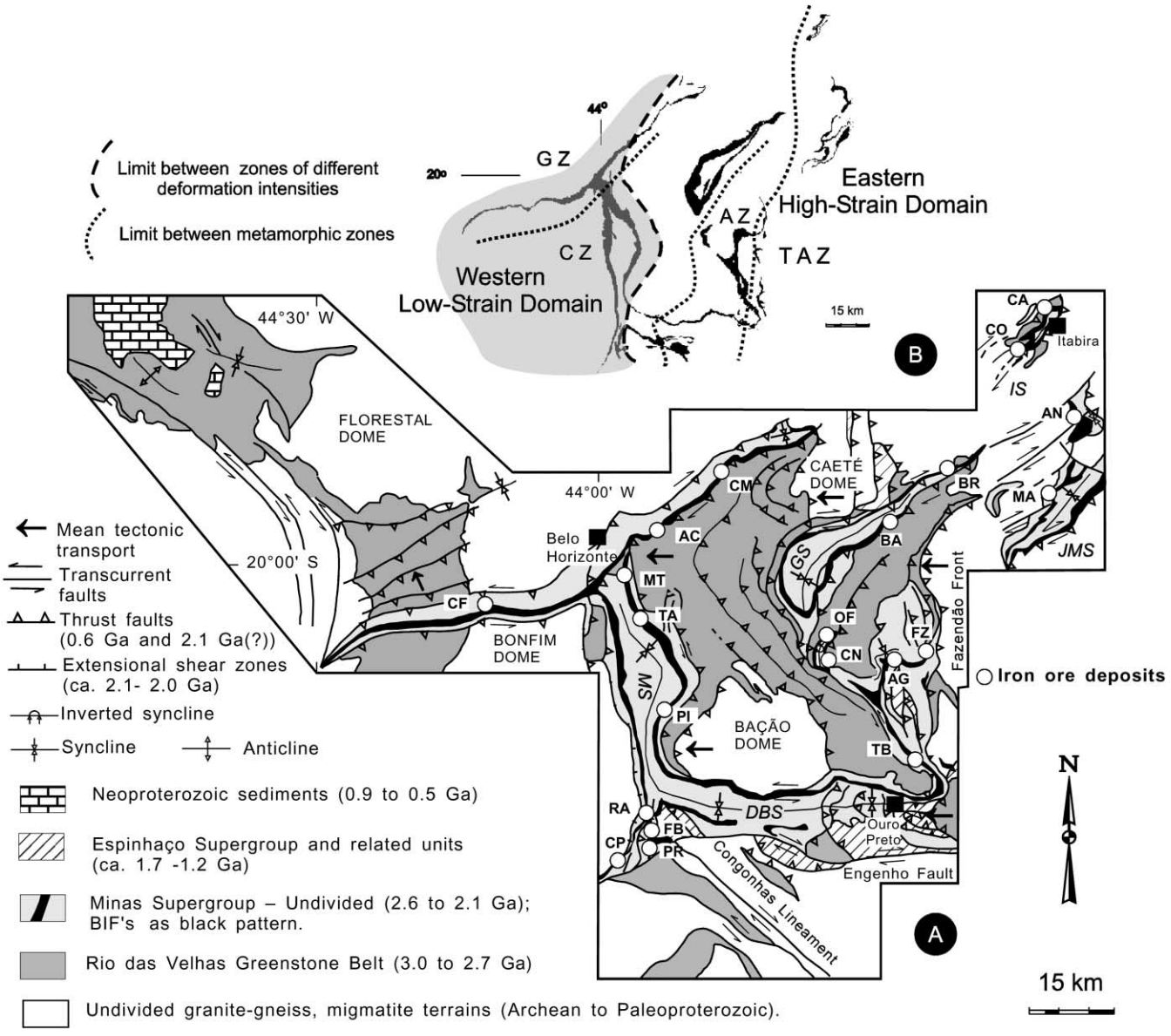

Fig. 1. (A) Geologic Map of the Quadrilátero Ferrífero (modified after Baars and Rosière (1997)). Major tectonic structures: DBS—Dom Bosco Syncline, MS—Moeda Syncline, GS—Gandarela Syncline, IS—Itabira Synclinorium, JMS—João Monlevade Synclinorium. Analyzed iron ore deposits: CF—Córrego do Feijão, MT—Mutuca, TA—Tamanduá, RA—Retiro das Almas, CP—Casa de Pedra, FB—Fábrica, PR—Pires, PI—Pico do Itabirito, AC—Águas Claras, CM—Córrego do Meio, OF—Ouro Fino, Capanema, CN—Capanema, TB—Timbopeba, AG—Alegria, FZ—Fazendão, BA—Baú, BR—Brucutú, MA—Morro Agudo, AN—Andrade, CO—Conceição, CA—Cauê. (B) Location of metamorphic and structural domains in the Quadrilátero Ferrífero. Shaded area depicts the low strain domain. Metamorphic zones after Pires (1995): GZ—Grunerite zone, CZ—Cummingtonite zone, AZ—Actinolite zone, TAZ—Tremolite–Anthophyllite zone. Depicted in black is the banded iron formation of the Itabira Group.

2. The Quadrilátero Ferrífero District and the structural setting of the iron ore deposits

The Quadrilátero Ferrífero district (Dorr, 1969), located at the southern border of the São Francisco Craton (Almeida, 1977), is characterized by a roughly quadrangular arrangement of synclines where Palaeoproterozoic platformal sediments of the Minas Supergroup outcrop, separated by irregular antiforms within Archean greenstone terrains of the Nova Lima Supergroup and Archean to Paleoproterozoic granite–gneiss domes (Fig. 1A). The Minas Supergroup comprises four sequences, namely, the Caraça, Itabira, Piracicaba and Sabará Groups (Dorr, 1969). The thickest sequences of banded iron formations with iron ore bodies belong to the Itabira Group and comprise itabirites, dolomites and subordinate metapelites. Itabirites (Eschwege, 1833) are strongly oxidized, metamorphosed banded iron formations presenting discontinuously distributed, more or less lenticular, hard, high-grade (>64% Fe) ore bodies with variable dimensions ranging from just a few centimeters up to hundreds of meters.

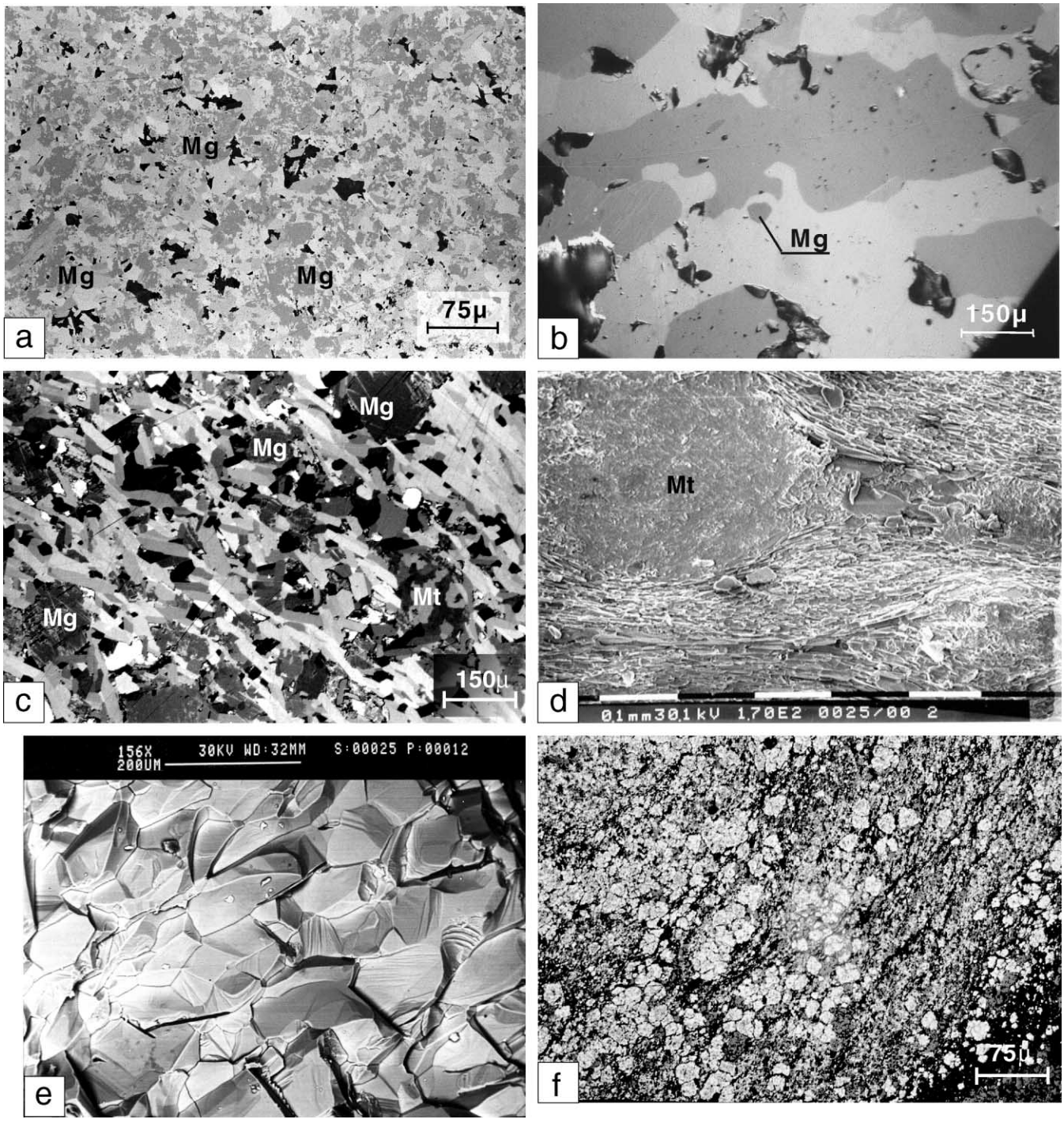

Fig. 2. Types of fabric in iron ores from the Quadrilátero Ferrífero. (a) Granoblastic magnetite/martite fabric of massive ore. Magnetite (Mg) appears in the Fe-deficient form kenomagnetite partially oxidized in martite. Sample TF16, Córrego do Feijão Mine (CF), AC-section. Reflected light, PPL. (b) Hematite crystals with lobate grain boundaries build a granoblastic fabric in strongly oxidized ore. A tiny relict of kenomagnetite (Mg) is still recognizable. Sample 57, Pico do Itabirito Mine (PI), AC-section Reflected light, partially XPL. (c) Granolepidoblastic fabric with a domainal schistosity defined by specularite plates enveloping granoblastic hematite/martite aggregates (Mt) and magnetite crystals (Mg). The schistosity is inclined about 45° to the banding that lies on the E–W direction of the photo. Sample TF1, Pires Mine (PR), AC-section. Reflected light, partially XPL. (d) Martite porphyroclast (Mt) surrounded by specularite. Elongated quartz and specularite crystals fill the strain shadows. Sample TF2, Retiro das Almas Mine (RA), SEM-image. (e) Mosaic granoblastic fabric of hematite. Sample TF25, Andrade Mine (AN), SEM-image. (f) Cataclastic deformed magnetitic-martitic iron ore. Small magnetite/martite aggregates are almost randomly distributed in a fine crushed hematite/martite matrix. Sample CF05, Córrego do Feijão Mine (CF). Reflected light, PPL.

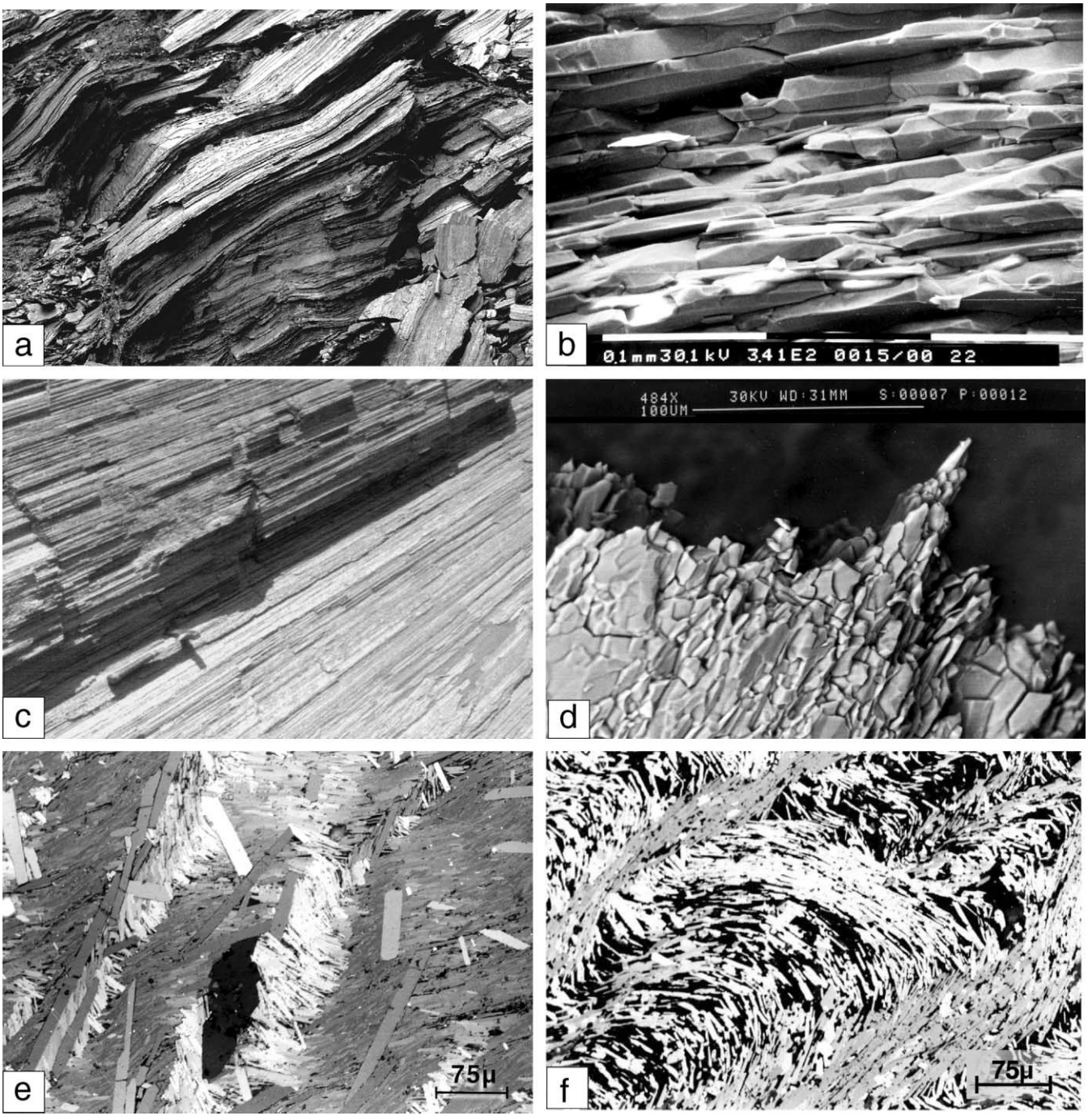

Fig. 3. Fabric of specularitic iron ores with well developed CPO. (a) Intense developed schistosity in iron ore, Conceição Mine (CO). (b) Schistose mylonitic ore with lepidoblastic fabric. The basal planes of the crystals define the foliation. Sample TF22, Andrade Mine (AN). SEM-image. (003) pole figure is defined by a single maximum. (c) Strongly lineated ore with fold axis rotated parallel to the mineral and stretching lineation defined by elongate specularite platelets. Morro Agudo Mine (MA) (d) Nematoblastic fabric with linear arrangement of specularite parallel to the stretching lineation. Sample TF7. Casa de Pedra Mine (CP), SEM-image. (003) pole figure is defined by a girdle. (e) and (f) Crenulated schistose iron ores. (003) pole figures are typical girdles. In (e), new specularite crystals grow along the axial plane cleavage of the microfolds. Sample TF12, Alegria Mine, section perpendicular to crenulation axis. Reflected light, partially XPL. In (f), there is a clear definition of the cleavage domains in contrast to the microlithon. Schistosity is disharmonically folded due to differential gliding. Sample from diamond drill hole CO159-438, 40 m, Conceição Mine, AC-section. Reflected light, partially XPL.

The regional structure developed from the superposition of two main deformational events (Chemale et al., 1994). The first event produced the nucleation of regional synclines on the supracrustal sequences and the uplift of the granite–gneiss domes during the Transamazonian Orogeny (2.1–2.0 Ga). The second event is related to a west-verging fold-thrust belt of Pan-African/Brasiliano age (0.8–0.6 Ga), causing inversion, amplification, translation and

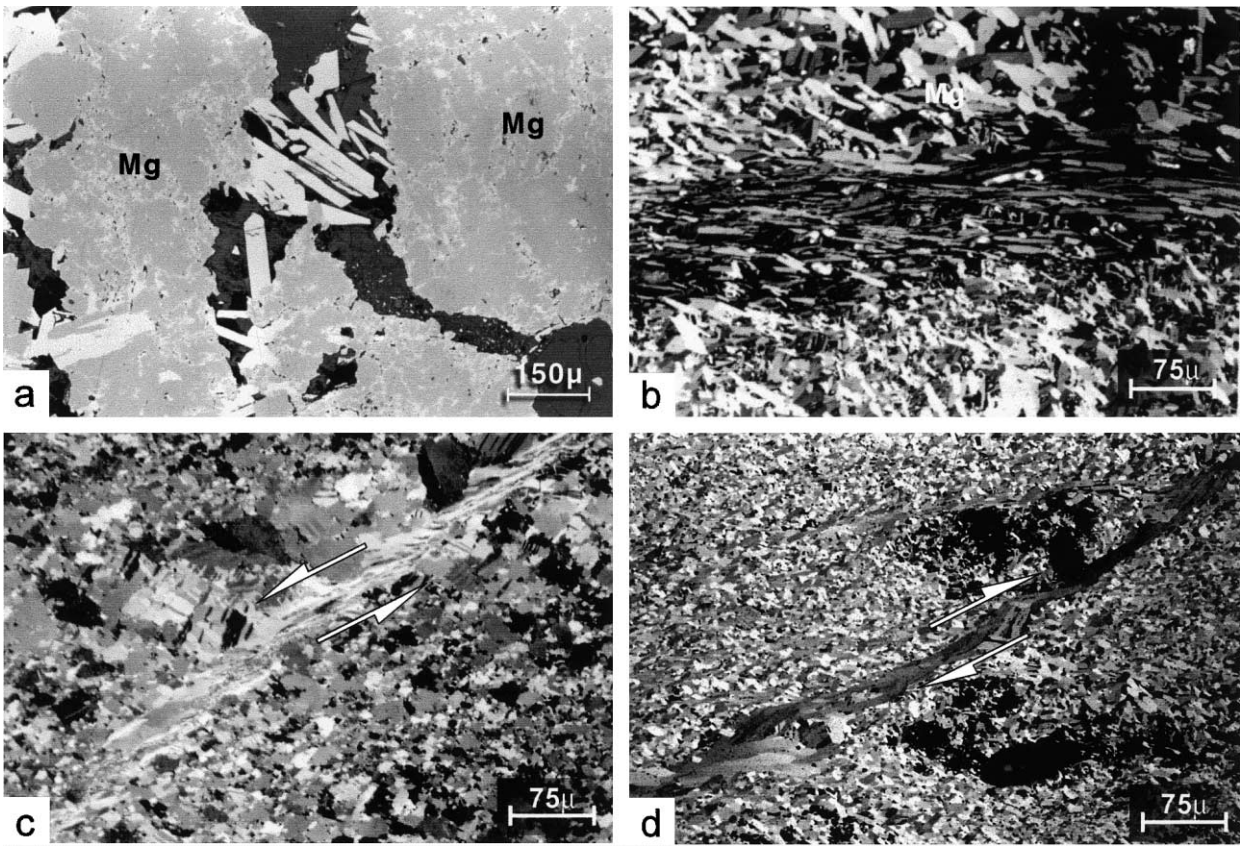

Fig. 4. Relationship between specularite and strain. (a) Specularite plates grown in extensional microfractures (dilational site) on magnetite (Mg) aggregates at the expenses of this mineral. This observation is in accordance with the Lagoeiro model (see text for further discussion). Sample TF32, Pico do Itabirito Mine (PI), BC-section. Reflected light, PPL. (b) Microscale shear zone with sigmoidal distribution of specularite crystals due to progressive orientation parallel to the shear zone. Sample TF32, Pico do Itabirito Mine (PI), AC-section. Reflected light, partially XPL. (c) and (d) Very similar, microscale shear zones developed in experimentally and naturally deformed granoblastic hematite ore with the growth of specularite plates on the shear plane. Reflected light, partially XPL. In (c), the shear zone developed in experimentally deformed ore and the movement is hanging-wall down (see arrows). Section perpendicular to banding and parallel to the $\sigma_1\sigma_3$ plane. σ_1 is in the vertical position. $T = 800°C$, $\epsilon = 20.6\%$, $d\epsilon/dt = 10^{-5}\ s^{-1}$, South African hematite ore. (d) Shear zone developed in naturally deformed ore. Sample TF14b, Fazendão Mine (FZ), AC-section. Arrows indicate shear sense. Dislocation is hanging-wall up. (b)–(d) support the hypothesis presented in this paper.

rotation of the synclines and is the reason for the development of the hematite textures.

This tectonic history produced a regional metamorphic zoning superimposed on the thermal aureoles around the domes (Herz, 1978; Marshak et al., 1992). Herz (1978) delineated isograds that separate three main zones (chlorite, biotite and staurolite) with eastwardly increasing equilibration temperatures that range from approximately 300 to 600°C. Pires (1995) redefined those isograds for pelitic rocks and iron formations of the Itabira Group, as presented in Fig 1B.

This metamorphic zoning is also accompanied by a deformational gradient such that it is possible to separate the Quadrilátero Ferrífero into two main structural domains (Fig. 1B). The western low-strain domain covers mainly the grunerite (GZ) and cummingtonite (CZ) metamorphic zones (Pires, 1995) and displays well-preserved megasynclines as the main regional structures. Discontinuous shear zones and thrust faults related to the second event intersect the megascopic structures. Iron formations preserve several sedimentary and diagenetic features like meso- and microbanding, pods formed by differential compaction and pisolites (Beukes, 1980). The eastern high-strain domain covers mainly the actinolite (AZ) and tremolite-anthophyllite (TAZ) metamorphic zones (Pires, 1995) and is dominated by thrusts and transcurrent shear zones generating tight to isoclinal folds and thick mylonitic zones (Chemale et al., 1994).

3. Microstructures and fabrics of iron ores

The main process controlling the development of microstructures in the itabirites from the Quadrilátero Ferrífero is the mineralogical change in the iron oxides (Rosière, 1981; Rosière and Chemale, 1991). Magnetite I is the earliest recognizable ore mineral and it appears as kenomagnetite (Kullerud et al., 1969; Morris, 1980; Rosière, 1981), a Fe^{2+}-deficient magnetite variety, as relics in martite and hematite aggregates (Fig. 2a and b). Kenomagnetite

oxidizes to martite and inverts to hematite that grows as xenoblastic to idioblastic crystals, denoted hematite II, III and IV (Hackspacher, 1979; Rosière, 1981; Rosière and Chemale, 1991), depending on its relationship to the main microstructural features of the ores. In deformed domains, partially or totally martitized magnetite displays cataclasis (Fig. 2f) and hematite appears as platy, elongated specularite crystals, which define the cleavage (Fig. 3a and b) and a conspicuous mineral lineation (Fig. 3c and d). With increasing proportions of specularite the fabric changes from granolepidoblastic to lepidoblastic or nematoblastic. Amphiboles and phyllosilicates may enhance the tectonic fabric. Quartz usually displays a fine polygonal granoblastic subfabric without shape-preferred orientation. The main types of cleavage are: (i) *spaced cleavage* defined by more or less discontinuous planes with specularite and platy minerals; (ii) *domainal cleavage* with anastomosing morphology defined by elongated xenomorphic hematite, martite or magnetite aggregates involved by specularite and platy minerals (Fig. 2c and d); (iii) *continuous cleavage* defined by the pervasive distribution of specularite, amphiboles or phyllosilicates (Fig 3a and b); and (iv) *crenulation cleavage* defined by microfolded specularite plates of the continuous schistosity with or without neoblastic specularite and platy minerals on the cleavage domains between the microlithons (Fig. 3e and f).

Oriented specularite also appears in veins and pressure shadows concentrated at the borders of magnetite porphyroclasts, as tabular grains together with elongated quartz crystals (Figs. 2d and 4a).

3.1. Regional distribution of specularite and its relation to strain and metamorphism in the Quadrilátero Ferrífero

The relationship between strain and formation of specularite cannot be quantified due to the lack of suitable strain markers in the itabirites, but a qualitative approach can be established based on the observations of the structures both in micro- and macroscopic scale. In the western low-strain domains of the Quadrilátero Ferrífero iron formations were deformed mainly by buckling with the local development of a tectonic foliation, and are cut by discrete brittle to ductile shear zones.

The overall fabric of the itabirite and high-grade bodies in the western domain is porous granoblastic, characterized by the presence of irregular aggregates of partially or totally martitized kenomagnetite, intergrown with xenoblastic to hypidioblastic hematite with no or very weak preferred orientation (Fig. 2a). Hematite grain boundaries are mostly irregular with lobate to embayed shapes (Fig 2b). In folded domains, specularite defines the axial planar foliation with the development of a spaced or a domainal cleavage (Fig. 2c). The intersection of the cleavage with the banding produces a conspicuous b-lineation, such as pencil structures or mullions.

In the extreme western part of the Quadrilátero Ferrífero, at the western limb of the Moeda Syncline (MS) and in the vicinity of the Córrego do Feijão Mine (CF) (Fig. 1A), brittle faults predominate. These appear as abrupt rupture planes or as relatively thick and diffuse zones presenting breccia or cohesive cataclasites (Fig. 2f). Cataclasites are composed of fine fragments of iron oxides, mostly magnetite or martite, resulting in a mesoscopically massive, apparently structureless, ore. In the eastern part of the low-strain domain, as at the eastern limb of the Moeda Syncline (MS) (Fig. 1A), discrete ductile shear zones are developed, where a lepidoblastic fabric of platy specularite crystals progressively substitutes the granoblastic hematite and delineates the strain trajectory (Fig. 4b).

With increasing strain, like that in flattened folds and ductile shear zones, foliation becomes more pervasive and the proportion of specularite increases, until primary banding is totally transposed and overprinted by the schistosity defined by phyllosilicates, amphiboles and specularite elongated plates with the development of a mineral lineation.

In the eastern high-strain domain, thick ductile shear zones are remarkable structural features in the BIFs. Deformation obliterates original banding resulting in thick bodies of S, S–L-tectonites (Fig. 3a and b) and subordinate L-tectonites (Fig. 3c and d) with nematoblastic fabrics. In iron ore deposits like Brucutú (BR), in the Gandarela Syncline (GS); Conceição (CO), in the Itabira Synclinorium (IS); and Andrade (AN) and Morro Agudo (MA) in the Monlevade Synclinorium (MS) (Fig. 1B), in the northeastern portion of the Quadrilátero Ferrífero, specularite prevails and the bodies acquire a homogeneous fabric. Foliation is continuous or anastomosed and specularite may involve 'porphyroclasts' of single magnetite/martite crystals and aggregates (Fig. 2d). Typical asymmetrically developed folds, strain shadows, hematite 'fish', microfaults in the porphyroclasts, and foliation inflection provide quite reliable shear sense indicators. Elongated plates and needles of specularite, together with porphyroclast strain shadows and pull-apart structures, define stretching lineations. Meter-size massive boudins with granoblastic fabric occur surrounded by a schistose specularitic matrix.

The strain gradient is followed by a metamorphic gradient (Fig 1B). Increasing temperature increases the ductility of the iron formations, promoting deformation, the development of specularite and also the growth of the platelets. In the grunerite and in the western cummingtonite zones (Pires, 1995), specularite plates, where present, are very fine, ranging from 10 to 70 μm long. In the eastern cummingtonite and into the tremolite–anthophyllite zone (Pires, 1995), the crystals attain 200 μm.

Temperature alone is not responsible for the development of specularite. Post-tectonic recrystallization, in contact-metamorphic zones, for instance, favors the development of a mosaic arrangement of hypidioblastic to idioblastic hematite grains with straight boundaries obliterating the former arrangement of the grains (Fig. 2e).

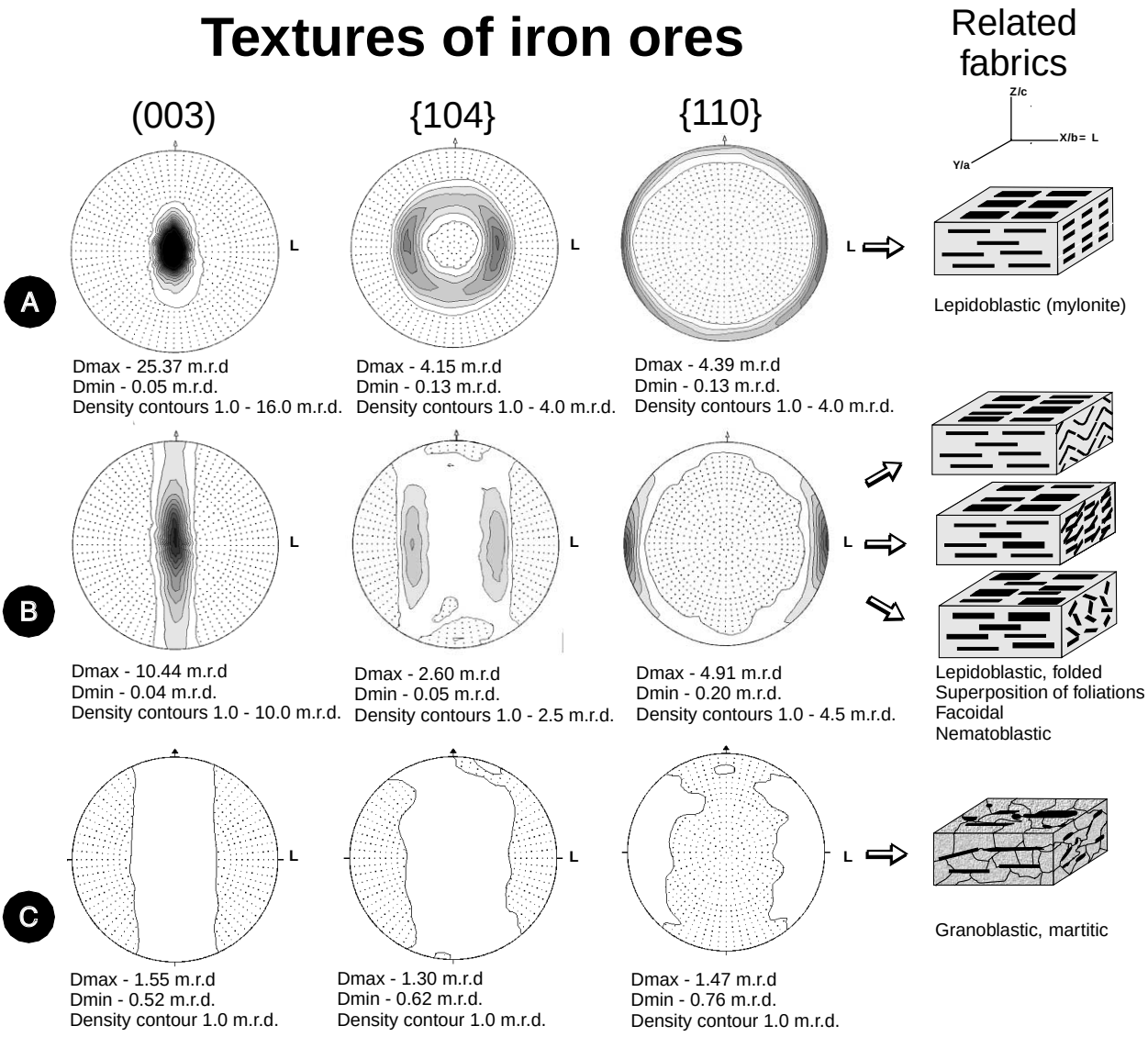

Fig. 5. (003), {104} and {110} pole figures of iron ores from the Quadrilátero Ferrífero and related fabrics. The projection planes of the stereograms are parallel to the mesoscopic most pervasive planar structure. L represents the orientation of the lineation. All diagrams have their lowest contour at 1.0 m.r.d. with 1.0 m.r.d. intervals. (a) Crystallographic preferred orientation related to lepidoblastic fabrics. Sample AC14-Andrade Mine (AN). (b) Crystallographic preferred orientation related to superposition of foliations, microfolded or crenulated schistosity or nematoblastic fabric. Sample AC47-Andrade Mine (AN). (c) Weakly developed crystallographic preferred orientation on martite granoblastic fabric of low-strain ores. The reference plane is the sedimentary banding. Sample TD4-Tamanduá Mine (TA).

4. Crystallographic preferred orientation of iron ores: description and interpretations

4.1. Methodological considerations: advantages of texture determination by neutron incidence

The CPO or texture of the trigonal hematite is usually measured by X-ray or neutron incidence. X-ray measurement yields only incomplete pole figures up to approximately 75–80° pole angles (e.g. Quade and Walde, 1982; Quade and Reinert, 1994; Bunge, 1997). In X-ray analysis, only a thin layer of material of a flat sample is irradiated, which for statistical reasons requires very fine grain sizes. Because of the inherent defocusing effects, the pole figures must be corrected, which is possible by different methods (e.g. Siemes et al., 2000). One way to obtain complete pole figures is to measure the intensities in three planes perpendicular to each other and to combine the three separate corrected, incomplete pole data (e.g. Hrouda et al., 1985; Rosière et al., 1998). Another possibility is to calculate the orientation distribution function (ODF) from several incomplete and corrected pole figures and to calculate the complete pole figures from the ODF (e.g. Bunge 1987; Schaeben and Siemes, 1996), but no example exists in the literature describing application of this method to hematite ores.

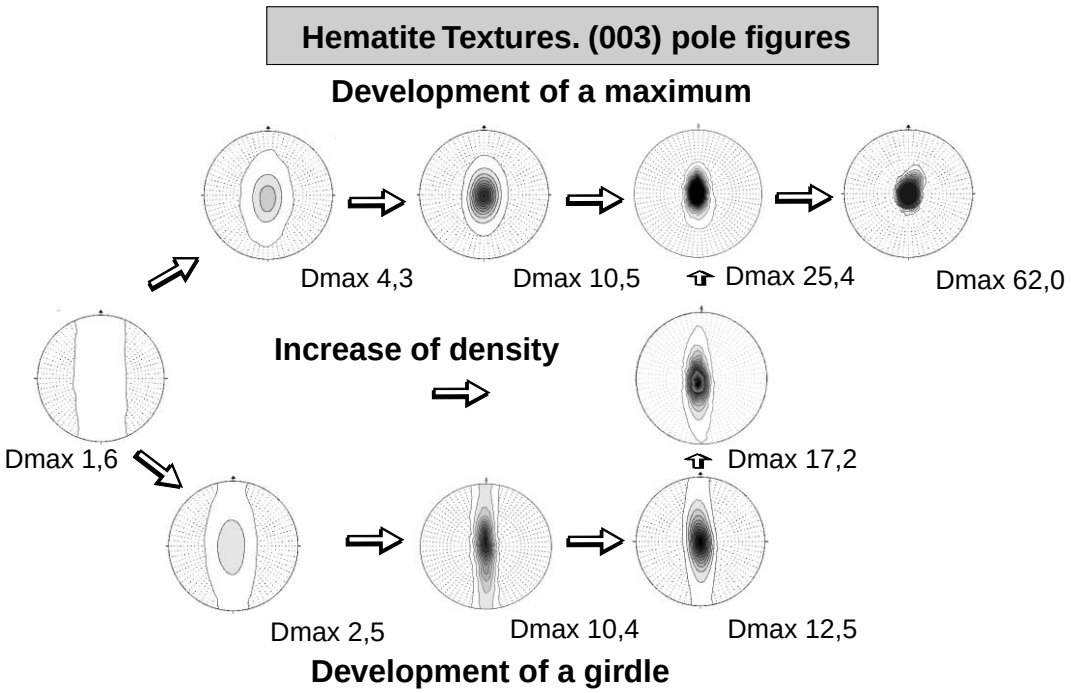

Fig. 6. Types of crystallographic preferred orientation in hematite ores according to the morphology of the (003) pole figures. The diagrams depicted on the upper row represents the maximum texture series while the lower row represents the girdle series. Both have their origin on a poorly recrystallized ore with a weakly developed crystallographic preferred orientation and converge into a high-density single maximum texture. All diagrams have their lowest contour at 1.0 m.r.d., with 1.0 m.r.d. intervals.

The advantages of neutron incidence for texture analysis are given in detail by Brokmeier (1994, 1999). The absorption of neutrons is lower than that of X-rays, typically by a factor of 10^2–10^4. That means that, in neutron analysis, the whole volume of a sample contributes to the diffracted intensity. On the other hand, the scattering factors for neutrons are much smaller. Hence, it is not only possible, but in most cases also necessary to use larger samples. The ideal shape of a sample for neutron texture measurement is the sphere. The reflection takes place in the whole volume of the sample and no correction for absorption, defocusing and other effects is necessary. The result is always a complete pole figure. Other sample shapes, such as cubes or cylinders, are usually satisfactory if the sample is completely irradiated by the neutron beam and the detector opening is large enough to accept the fully diffracted beam.

The large sample size permits the statistically significant detection of a global, preferred orientation and especially very weak textures which cannot be detected by X-ray incidence (e.g. Siemes et al., 1993). The large sample size in connection with the low absorption permits the measurement of textures of several components (e.g. Brokmeier, 1999) in a multiphase sample. The non-destructive measurement is very suitable for determining a texture before and after a treatment such as deformation (e.g. Jansen et al., 1998), recrystallization or phase change depending on external parameters (e.g. Wagner et al., 1977). The scattering factors for neutrons do not show the systematic variation with atomic number as in the case of X-rays. As a consequence of these different scattering factors of the atoms, the structural factors of a crystalline phase are also different. Therefore, the reflected intensities of the same crystallographic plane may be strongly different in X-ray and neutron diffraction.

Besides the reflections from the interactions with the nuclei, magnetic reflections are possible, and/or mixtures of both. This is because part of the scattering of neutrons takes place by a magnetic interaction between the spin of the neutron and the spin of the electrons. Thus, the reflected neutron intensity can depend on the magnetization of the sample. This is especially interesting for hematite because, in X-ray diffraction, the (006)-pole figure is very difficult to measure due to its low intensity ($<3\%$). In neutron diffraction, the magnetic (003)-reflection intensity is in the order of 50% and can be measured easily.

4.2. Hematite textures

The complete pole figures representing textures of naturally deformed iron ores from the Quadrilátero Ferrífero were obtained with the neutron goniometer TEX2 (Brokmeier et al., 1998) at the Research Center GKSS Geesthacht, Germany, on samples from areas of different intensities of deformation and metamorphism. A few representative pole figures measured on three different crystallographic planes: (003)-basal plane; {110}-prism and {104}-rhombohedron, are presented in Fig. 5. Further examples are published by Quade et al. (2000). The samples

were oriented according to the prevailing s-surface and to the lineation. In low-strain domains, this surface corresponds to the primary banding and, in high-strain domains, to the schistosity; this surface was taken as the reference plane. The character of the lineation is also different depending on the magnitude of deformation. In low-strain domains, it corresponds to an intersection lineation and in high strain domains the lineation is defined by the long axis of elongated specularite plates, usually parallel to the stretching direction. In the former case the *a*–*b*–*c* geometric notation is used and, in the latter, the *X*–*Y*–*Z* strain notation is used.

Strong preferred orientations are characteristic for highly strained hematite ores. The measurements have shown that there is a continuous variation between the different textures from the analyzed samples, thereby constituting a texture series (Fig. 6). At one extreme of this series are the single, circular to elliptical (003) pole maxima, which coincide with the foliation pole and represent the highest degree of lattice preferred orientation of the ores with densities as high as 62 m.r.d. (multiples of random distribution). The corresponding {110} texture is characterized by a girdle parallel to the main foliation with a single maximum up to 6 m.r.d. centered on the mineral lineation. Pole figures of the {100}-prism reveal the same maxima in the same orientation, which is the result of the degree of freedom for rotation of the *a*-axes around the *c*-axis of the hematite crystals (Siemes and Hennig-Michaeli, 1985; Will et al., 1990; Wenk, 1998). The {104} pole figures show the configuration of a round cleft girdle with elongated 'banana-shaped' maxima (Quade, 1988) (Fig. 5a). The concentration of the densities may vary without changing the shape of the pole figures.

With the increase of the ellipticity of the (003) maximum, a girdle perpendicular to the lineation develops, followed by an elongation of the {104} maxima and a relative decrease of the densities. The {104} 'butterfly diagram' (Quade, 1988) corresponds to the case of extreme ellipticity of the (003) maximum. The girdle of the {110} planes is broadened but the maximum does not necessarily decrease in its relative density (Fig. 5b). Weakening on the other planes follows a further decrease in density of the (003) girdles, although the position of the maxima in relation to the fabric coordinates remains unchanged.

At the opposite extreme of the series are the nearly random distributions or very weak textures that are characteristic for porous granoblastic ores with high martite content (Fig. 5c) that underwent only low strains or cataclastic deformation.

Pole figures of the (003) reflection are the most suitable to quantify the degree of preferred orientation of the basal plane of specularites and, consequently, the development of schistosity and the intensity of its maximum can be directly related to the magnitude of deformation. Maximum textures represent typical lepidoblastic fabrics developed in shear zones (Fig. 5a). Elongated single maxima develop into girdles associated with different types of fabrics (Fig. 5b):

1. Nematoblastic fabrics, where poles of the basal plane are distributed in a plane perpendicular to stretching direction;
2. Microfolded or crenulated schistosity; and
3. Interference of foliations.

Nematoblastic fabrics only occur locally, but in contrast, folds on different scales are the most common features in the iron formations. This fact leads us to conclude that girdle stereograms of the basal plane can be considered typically related to nucleation of these structures. Orientation of specularite in the axial planar schistosity interferes with hematite crystals on the banding planes that results in the single maximum encountered on the {110} pole figures coinciding with the fold axis. Progressive flattening or shearing once again increases the strength of the concentration of the (003) poles into a single maximum. Late crenulations further modify the texture scattering the reflections again along a girdle perpendicular to the fold axis.

In weakly deformed ores, pole figures display the same geometric features as those of the textures related to folding, although, with much lower densities on the reflections (Fig. 5c). The constant parallelism between the pole maximum of the {110} and {100} planes, the trend of the maxima presented by the {104} planes, and the orientation to the lineation, regardless of its origin (stretching lineation in shear zones or intersection lineation in folded ores), indicate that this structure is an important constraint in the development of textures both under high and low strains. A feasible interpretation for this feature is that, during the structural development of iron ores, strain tends to be partitioned by slip along the banding or along the foliation, resulting in a continuous and disharmonic nucleation of intrafolial folds, whose axes are progressively rotated into the stretching direction. This conclusion coincides with field and polished section observations in previous publications (e.g. Guba, 1982; Ladeira and Viveiros, 1984) that describe superposition of folds on different scales as a common feature.

In summary, two main types of deformation textures can be separated according to the morphology of the (003) pole figures. Each one represents a variant of the texture series that develops under different conditions and whose density increases proportionately to the magnitude of deformation (Fig. 6):

1. More or less elliptical to circular maximum textures.
2. 180° girdles.

The first variant develops in shear zones with progressive formation of specularite parallel to foliation, while the second is related to folding that may further develop into a single maximum texture due to progressive flattening of the structures.

5. Discussion of the deformation mechanisms

Iron formations and ores from the western domain of the Quadrilátero Ferrífero are weakly strained or deformed in a cataclastic process. Observation of the microstructures from this domain allows us to conclude that magnetite had an important influence on the mechanical behavior of the iron formations prior to its oxidation and transformation to hematite. Magnetite behaved with relative competence and brittleness, probably under the influence of high fluid pressure and deformation accommodated by cataclastic flow. The origin of the fluid is still uncertain but it was probably responsible for the intensive oxidation of magnetite (martitization) and the production of quartz and hematite veins that commonly cement breccia and cataclasites. These cataclastic structures must have developed very early in the tectonic history of the Quadrilátero Ferrífero, possibly during the first deformation event (Chemale et al., 1994) and remained relict in the western domain. After magnetite was almost completely oxidized, deformation was controlled solely by the behavior of hematite and its interaction with the gangue minerals (quartz and carbonates).

Hematite from iron ore in low-strain domains of the Quadrilátero Ferrífero does not display grain-shape preferred orientation and shows weakly developed textures (e.g. Fig. 2a). In folded samples, deformation seems to be accommodated by the gliding of the single layers along their boundaries. Increasing strain by progressive flattening or shearing of the iron formations and high-grade ores promotes the formation of specularite and the simultaneous development of a crystallographic preferred orientation.

It seems that the formation of specularite crystals is an important softening mechanism in the deformation of iron ores. This is attested by the observation of the boudins of hard, massive, high-grade ore as described above. To explain the formation of specularite or why hematite grows as oriented platy crystals, two main hypotheses can be considered, both using variation in the strain energy as the driving force for the processes.

The first hypothesis explains the formation of specularite by solution-precipitation processes associated with oxidation of magnetite (martitization) during metamorphism. Oxidation of magnetite to kenomagnetite and martite starts along {111} planes enhanced by high dislocation density followed by fluid penetration and dissolution of Fe^{2+} in a similar manner to that proposed by Davis et al. (1968) and Morris (1983), although under the influence of metamorphic fluids. Fe^{2+} reacts with oxygen and precipitates as specularite at oxidizing sites along magnetite grain boundaries parallel to the foliation, particularly in strain shadows and veins (Fig. 4a). The progressive transformation and precipitation leads to a penetrative foliation defined by specularite plates. Lagoeiro (1998) advocates this mechanism alone as responsible for the formation of specularite in the itabirite.

The second hypothesis associates specularite with crystal plastic deformation of hematite by dislocation glide on the basal plane, followed by recrystallization and anisotropic grain growth driven by the differential of strain energy between deformed crystals. Hematite crystals may have been rotated into favorable positions for preferential basal gliding, in order to promote the growth of grains parallel to the tectonic s-plane at the expense of others that had acquired a higher dislocation density.

5.1. Experimental deformation results

Deformation experiments with emphasis on the development of the microstructure and the crystallographic preferred orientation on coarse-grained hematite at temperatures between 25 and 450°C and strain rates between 10^{-4} and $10^{-5}\,s^{-1}$ are described by Hennig-Michaeli (1977) and on fine-grained hematite at temperatures between 600 and 1100°C and strain rates between 10^{-4} and $10^{-6}\,s^{-1}$ by Siemes et al. (1999a,b) and Siemes and Klinkenberg (2000). At low temperatures, microfracturing and r-twinning, as well as c-twinning and $\{a\} < m >$ slip (Hennig-Michaeli and Siemes, 1982) are the main deformation mechanisms. Above 600°C, prism $\{a\} < m >$ slip is the preferential glide system with only a few r-twins recognizable, while above 800°C, the importance of basal glide $(c) < a >$ increases. Recovery and recrystallization initiate above 900°C. At the highest experimental temperatures, indications of diffusional flow processes are detectable. In all experiments, the development of the crystallographic preferred orientation was controlled by neutron-incidence texture analysis of the samples before and after deformation. Depending on the orientation of the compression axis to the original weak preferred orientation, {100} and (001) maxima develop at low temperatures, whereas at temperatures beginning at 800°C, the development of a (001)-maximum is the most prominent feature.

5.2. Comparison between nature and experiments—concluding remarks

Our observations on naturally deformed metamorphic ores from the Quadrilátero Ferrífero are in agreement with the experimental results. In order to make use of the experimental data for the interpretation of naturally deformed ores, one has to bear in mind some severe differences that exist between nature and experiment. The deformation experiments are coaxial, whereas the deformation suffered by the itabirite is dominantly non-coaxial and preferentially occurred by simple shear (Chemale et al., 1994). Geological strain rates are of the order of $10^{-14}\,s^{-1}$, which is not comparable with the experimental strain rates but, as Paterson (1976) points out, experiments at higher temperatures deliver valuable information on the behavior of materials at strain rates below the experimental limitations.

The weak crystallographic preferred orientation found in hematite ores in low-strain domains of the Quadrilátero Ferrífero leads us to suppose that basal planes might be

easily activated under geological conditions at temperatures between 300 and 600°C, clearly below the experimental temperatures of 600–1100°C, possibly also helped by hydrolithic weakening. Deformation twins are almost totally absent in the ores from the Quadrilátero Ferrífero and they can be found only in hematite, along younger, brittle faults. At the prevailing temperatures and strain rates, twins could not occur, or they might have been obliterated by later recrystallization.

It seems reasonable to accept the hypothesis that the activation of the basal-plane glide system results in the development of specularite platelets that will be easily rotated into the principal deformation plane as they grow. The formation of platy specularite crystals as markers for the shear plane is confirmed by the striking similarity between micro-shear zones at the scale of polished sections found both in naturally and experimentally deformed ores (Fig. 4c and d). If the basal planes of the specularite crystals are allowed to rotate freely during deformation, they will do so around an axis perpendicular to any of the prismatic faces resulting in maxima parallel to stretching lineation. This is found in the {110} and {100} pole figures that accompany the girdle distribution of the (003) pole figures (Fig. 5b).

After the total transformation to specularite, the final schistose hematite fabric can be further deformed by intercrystalline glide on the foliation plane in a flexural slip mechanism promoting rigid body rotation and basal gliding on the specularite plates, resulting in crenulations and intrafolial folds (Fig. 3e and f). Recrystallization of high-strained crystals and further anisotropic grain growth of deformed and/or rotated plates results in a domainal type of crenulation foliation with microfolded microlithons alternating with domains defined by parallel reoriented specularite crystals.

Dislocation gliding on the basal plane followed by grain boundary migration recrystallization and anisotropic grain growth was certainly not the sole process responsible for the formation of specularite in the itabirites of the Quadrilátero Ferrífero, but it was very important as a deformation mechanism of regional significance in the control of the ductile behavior of the iron formations, particularly under higher strains.

Solution precipitation processes assisted by fluids, as proposed by Lagoeiro (1998), in contrast, involve a strong mobilization of cations and the occupation of dilational sites or empty space left by the solution of gangue minerals, like quartz or carbonates. This process is also conditioned to the amount of strain in the iron formations and worked in the itabirites of the Quadrilátero Ferrífero complementary to the ductile behavior of hematite whenever magnetite relicts were present. The local predominance of this process must allow the remobilization of considerable amounts of iron and probably resulting in the formation of some important syntectonic schistose, specularitic high-grade bodies present in the Quadrilátero Ferrífero, like in the Conceição and Timbopeba deposits (Fig. 1A).

The endurance of the temperature after deformation in the Quadrilátero Ferrífero resulted in post-tectonic recrystallization and secondary grain growth that did not affect the textures developed during deformation. Granoblastic ores with mosaic fabric also show a very high degree of crystallographic preferred orientation. This fabric is also present in the experiments at temperatures above 900°C (Siemes et al., 1999a; Siemes and Klinkenberg, 2000).

The present results of this research permit a better insight into the problems related to the deformation of iron ores and how to interpret their microstructures in relationship to the regional tectonic development. The formation of specularite played an important role in the behavior of the iron ores, in the development of several generations of tectonic structures and in the concentration of rich bodies that will be the subject of further papers.

Acknowledgements

The authors wish to thank the FINEP, CAPES, DAAD, DFG and CNPq for financial support, the mining companies CVRD, MSG, FERTECO, MBR, CSN and SAMITRI for providing logistical support and access to their industrial facilities. We express our special thanks to the geologists Aércio Januzzi, Nelson Borges, Diniz Tamantini, Edson Albanez and Leonardo Lagoeiro for valuable discussions. We thank also F. Baars, H. Dayan, T. Blenkinsop, G. Dresen and an anonymous reviewer for the suggestions that permitted a substantial improvement of the original text.

References

Almeida, F.F.M., 1977. O Cráton de São Francisco. Revista Brasileira de Geociências 7, 349–364.

Baars, F.J., Rosière, C.A., 1997. Geological map of the Quadrilátero Ferrífero. In: Baars, F.J. The São Francisco Craton. In: De Wit, M.J., Ashwal, L.A. (Eds.). Greenstone Belts, Oxford Monographs on Geology and Geophysics Series, Oxford University Press, pp. 529–557.

Beukes, N.J., 1980. Suggestions towards a classification of and nomenclature for iron-formation. Transactions of the Geological Society of South Africa 83, 285–290.

Brokmeier, H.-G., 1994. Application of neutron diffraction to measure preferred orientations of geological materials. In: Bunge, H.-J., Skrotzki, W., Siegesmund, S., Weber, K. (Eds.). Textures of Geological Materials. DGM Informationsgesellschaft, Oberursel, pp. 327–344.

Brokmeier, H.-G., 1999. Advantages and Applications of Neutron Texture Analysis. Textures and Microstructures 33, 13–34.

Brokmeier, H.-G., Zink, U., Schnieber, R., Witassek, B., 1998. TEX-2, Texture Analysis at GKSS Research Center (Instrumentation and Application). In: Schwarzer, R. (Ed). Texture and Anisotropy of Polycrystals. Materials Science Forum 273–275, 277–282.

Bunge, H.-J., 1987. Three-dimensional texture analysis. International Materials Reviews 32, 265–291.

Bunge, H.-J., 1997. X-ray texture analysis in materials and earth sciences. European Journal of Mineralogy 9, 735–761.

Chemale Jr., F., Rosière, C.A., Endo, I., 1994. The tectonic evolution of the Quadrilátero Ferrífero, Minas Gerais, Brazil. Precambrian Research 65, 25–54.

Davis, B.L., Rapp Jr., G., Walawender, M.J., 1968. Fabric and structural

characteristics of the martitization process. American Journal of Science 266, 482–496.

Dorr II, J.N., 1965. Nature and origin of the high grade hematite ores of Minas Gerais, Brazil. Economic Geology 60, 1–46.

Dorr II, J.N., 1969. Physiographic, stratigraphic and structural development of the Quadrilátero Ferrífero, Minas Gerais. United States Geological Survey Professional Paper, 641-A.

Eschwege, W.L.v., 1833. Pluto Brasiliensis. Verlag G. Reimer, Berlin.

Guba, I., 1982. Tektonik, Texturen und Mineralogie der Präkambrischen Eisenerze und Nebengesteinsserien der Lagerstätte Morro Agudo im NE des Quadrilátero Ferrífero/Minas Gerais, Brasilien. Dissertation, Technische Universität Clausthal, Clausthal-Zellerfeld.

Guild, P.W., 1957. Geology and mineral resources of the Congonhas District, Minas Gerais, Brazil. United States Geological Survey Professional Paper, 290.

Hackspacher, P.C., 1979. Strukturelle und Texturelle Untersuchungen zur internen Deformation des Eisenreicherzkörpers der Grube "Águas Claras" bei Belo Horizonte, Minas Gerais, Brasilien. Clausthaler Geologische Abhandlungen 34, Clausthal-Zellerfeld.

Hennig-Michaeli, C., 1977. Microscopic structure studies of experimentally and naturally deformed hematite ores. Tectonophysics 39, 255–271.

Hennig-Michaeli, C., Siemes, H., 1982. Experimental deformation of hematite crystals between 25°C and 400°C at 400 MPa confining pressure. In: Schreyer, W. (Ed.). High Pressure Researches in Geoscience. E. Schweizerbart, Stuttgart, pp. 133–150.

Herz, N., 1978. Metamorphic rocks of the Quadrilátero Ferrífero, Minas Gerais, Brazil. United States Geological Survey Professional Paper, 641-C.

Hrouda, F., Siemes, H., Herres, N., Hennig-Michaeli, C., 1985. The relationship between the magnetic anisotropy and the *c*-axis fabric in a massive hematite ore. Journal of Geophysics 65, 174–182.

Jansen, E.M., Siemes, H., Brokmeier, H.-G., 1998. Crystallographic preferred orientation and microstructures of experimentally deformed Braubach galena ores with emphasis on the relation to diffusional processes. Mineralium Deposita 34, 57–70.

Kullerud, G., Donnay, G., Donnay, J.D.H., 1969. Omission solid solution in magnetite: Kenotetrahedral magnetite. Zeitschrift für Kristallographie 128, 1–17.

Ladeira, E.A., Viveiros, J.F.M., 1984. Hipótese sobre a estruturação do Quadrilátero Ferrífero com base nos dados disponíveis. Boletim da Sociedade Brasileira de Geologia, Núcleo Minas Gerais 4, Belo Horizonte.

Lagoeiro, L.E., 1998. Transformation of magnetite to hematite and its influence on the dissolution of iron oxide minerals. Journal of Metamorphic Geology 16, 415–423.

Marshak, S., Alkmim, F.F., Jordt-Evangelista, H., 1992. Proterozoic crustal extension and the generation of dome-and-keel structure in an Archean granite greenstone terrain. Nature 357, 491–493.

Morris, R., 1980. A textural and mineralogical study of the relationship of iron ore to banded iron formation in the Hamersley Iron Province of Western Australia. Economic Geology 75, 184–209.

Morris, R., 1983. Supergene alteration of banded iron formation. In: Trendall, A.F. (Ed.). Iron formation Facts and Problems, Developments in Precambrian Geology, vol. 6. Elsevier, Amsterdam, pp. 513–532.

Paterson, M.S., 1976. Some current aspects of experimental rock deformation. Philosophical Transactions of the Royal Society London A283, 163–172.

Pires, F.R.M., 1995. Textural and mineralogical variations during metamorphism of the Proterozoic Itabira Iron Formation in the Quadrilátero Ferrífero, Minas Gerais, Brazil. Anais da Academia Brasileira de Ciência 67 (1), 77–105.

Quade, H., 1988. Natural and simulated (10.4) pole figures of polycrystalline hematite. Texture and Microstructures 8–9, 719–736.

Quade, H., Walde, R., 1982. Texturuntersuchungen an hämatitischen Reicherzen. Archiv für das Eisenhüttenwesen 53, 85–89.

Quade, H., Reinert, T., 1994. Magnetic anisotropy and texture of banded hematite ores. Materials Science Forum 175–162, 1681–1688.

Quade, H., Rosière, C.A., Siemes, H., Brokmeier, H.-G., 2000. Fabrics and textures of Precambrian iron ores from Brazilian deposits. Zeitschrift für angewandte Geologie, Sonderheft 1, 155–162.

Rosière, C.A., 1981. Strukturelle und texturelle Untersuchungen de Eisenerzlagerstätte "Pico de Itabira" bei Itabirito/Minas Gerais, Brasilien. Clausthaler Geowissenschaftliche Dissertationen 9, Clausthal-Zellerfeld.

Rosière, C.A., Quade, H., Siemes, H., Chemale Jr, F., 1998. Fabric, texture and anisotropy of magnetic susceptibility in high-grade iron ores from the Quadrilátero Ferrífero, Minas Gerais, Brazil. Materials Science Forum 273–275, 693–700.

Rosière, C.A., Chemale Jr, F., 1991. Textural and structural aspects of iron ores from Iron Quadrangle, Brazil. In: Pagel, M., Leroy, J.L. (Eds.). Source, Transport and Deposition of Metals. Balkema, Amsterdam, pp. 485–488.

Schaeben, H., Siemes, H., 1996. Determination and interpretation of preferred orientation with texture goniometry: an application of indicators to maximum entropy pole- to orientation-density inversion. Mathematical Geology 28, 169–201.

Siemes, H., Hennig-Michaeli, C., 1985. Ore minerals. In: Wenk, H.-R. (Ed.). Preferred Orientation in Deformed Metals and Rocks, an Introduction to Modern Texture Analysis. Academic Press, Orlando, pp. 335–360.

Siemes H., Klingenberg, B., 2000. Analyse der Entwicklung der mit Neutronenbeugung gemessenen Texturen und des Mikrogefüges von experimentell verformten polykristallinen Hämatit. Unpublished DFG Final Report, available from H.S., 36 + 68p.

Siemes, H., Zilles, D., Cox, S.F., Merz, P., Schäfer, W., Will, G., Schaeben, H., Kunze, K., 1993. Preferred orientation of experimentally deformed pyrite measured by means of neutron diffraction. Mineralogical Magazine 57, 29–43.

Siemes, H., Klingenberg, B., Dresen, G., Rybacki, E., Naumann, M., Schäfer, W., Jansen, E., 1999a. Microstructure and texture of experimentally and naturally deformed hematite ores. In: Dresen, G., Handy, M., Janssen, C. (Eds.). Abstracts of the International Conference on Deformation Mechanisms, Reology, Microstructures, p. 138 Neustadt a. d. Weinstr., 22–24 March 1999.

Siemes, H., Klingenberg, B., Dresen, G., Rybacki, E., Naumann, M., Schäfer, W., Jansen, E., Rosière, C.A., 1999b. Experimentally and naturally deformed hematite ores. Anais do VII Simpósio Nacional de Estudos Tectônicos 1999, Lençois (Bahia), Brasil. Sessão 5, 59.

Siemes, H., Rosière, C.A., Hackspacher, P., Schäfer, W., Jansen, E., 2000. Defocusing correction of X-ray pole figures by means of neutron pole figure measurement. Textures and Microstructures 34, 55–62.

Wagner, F., Esling, C., Baro, R., Englander, M., 1977. Textures of iron oxide ores by neutron diffraction and topotactical relation. Zeitschrift für Metallkunde 68, 701–704.

Wenk, H.-R., 1998. Typical textures in geological materials and ceramics. In: Kocks, U.F., Tomé, C.N., Wenk, H.-R. (Eds.). Texture and Anisotropy. Cambridge University Press, Cambridge, pp. 240–280.

Will, G., Merz, P., Schäfer, W., Dahms, M., 1990. Application of position sensitive detectors for neutron diffraction texture analysis of hematite ore. In: Barret, C.S., Gilfrisch, J.V., Huang, T.C., Jenkins, R., Predecki, P.K. (Eds.). Advances in X-Ray Analysis, vol. 33. Plenum Press, New York, pp. 277–283.